

## Active Surgeon Support during Orthopedic Surgery using the BOrESCOPE-Exoskeleton: System Design and First Results

Peter P. Pott, Markus Hessinger, Roland Werthschützky, Helmut F. Schlaak  
 Institute of Electromechanical Design  
 Technische Universität Darmstadt  
 Darmstadt, Germany  
 p.pott@emk.tu-darmstadt.de  
 m.hessinger@emk.tu-darmstadt.de  
 werthschuetzky@emk.tu-darmstadt.de  
 schlaak@emk.tu-darmstadt.de

Eugen Nordheimer, Essameddin Badreddin, Achim Wagner  
 Institute of Computer Engineering, Automation Lab  
 Heidelberg University  
 Heidelberg, Germany  
 eugen.nordheimer@ziti.uni-heidelberg.de  
 badreddin@ziti.uni-heidelberg.de  
 achim.wagner@ziti.uni-heidelberg.de

**Abstract**— A great number of medical robotics projects is driven by researchers all around the globe. Aim is to enhance surgery output, accelerate the procedure or to shorten post-operative convalescence. In most cases, the surgeon interacts with a machine directly by some kind of remote control in general soft tissue surgery or robotic systems recapitulate pre-programmed trajectories, e.g., during milling of cavities. One option to achieve a better acceptance in human robot interaction systems in operating theatre is to use exoskeletons for tight integration. This is widely accomplished in body rehabilitation to provide patients with continuous passive or active motion. However the way to commercial application is long for many systems. In this paper for an anthropomorphic upper extremity exoskeleton worn by the surgeon during orthopedic interventions (e.g., pedicle drilling) first results concerning control strategy and user guidance are presented. The system is intended to enhance overall task-precision as the surgeon is guided by optic, acoustic, and haptic perception. The parallel flux of forces and the inherently wearable robot base attached to his back allow the surgeon to directly maintain responsibility for surgery. The mechanical design as well as the control strategy are described briefly. The device provides seven concentric axes and uses conventional DC motors and wire gears to deliver torque. An optical tracking system is employed to provide low-latency absolute position data of the system and the patient. A User Guidance Opto-Acoustic Display is utilized to provide the surgeon with information on position and orientation of the tool in six degrees of freedom with respect to the desired trajectory. The control strategy is decomposed into several levels. First experiments have demonstrated the correlation between provided workspace and space requirements during pedicle screw placement and an intuitive handling of the user guidance system to follow a desired trajectory.

**Keywords**- *exoskeleton, orthopedic surgery, human-machine interaction, behavior-based system decomposition*

### I. INTRODUCTION

Parts of this work have been previously published at the 7<sup>th</sup> International Conference on Advances in Computer-Human Interactions (ACHI 2014), March 23-27 2014, Barcelona, Spain [1].

Medical robotic systems for the use in the OR have been under development for more than 20 years [2]. Early systems for neurosurgery [3] [4] and orthopedics [5] proved usefulness and even made it for commercialization. However, their impact was not as high as expected [6]. In the last ten years, many new robotic systems have been developed and even introduced to the market. The most successful is the daVinci Surgical System by Intuitive Surgical, Inc., Sunnyvale, CA, USA. Nevertheless, there are hundreds of different systems [2] and many specific reviews e.g., by Nguyen [7], Taylor and Stoianovici [8], Cleary and Stoianovici [9], Korb [10], Cepolina [11], Kuo [12], Vitiello [13], Dhumane [14] to learn more about the various fields of robotics.

The aim of our work is to develop and to design a robotic interaction system for orthopaedic surgery. Here, the surgeon has to fulfil delicate tasks like drilling the spine while maintaining high precision in the sub-millimetre range. Placing a cooperating robotic arm next to the OR table [15], the ceiling [16] or even on the patient [17] does not seem to be appropriate. The primary reason is that such systems either require rather large space next to the table, have to be rigidly installed in the OR reducing flexibility of use, or tend to hinder the approach to the situs due to their mounting in the third case. Earlier work of our group showed the high potential of placing the robot in the user's hand [18] [19] to compensate tremor and involuntary movements both from surgeon and patient [20]. This robotic system provides precise movement and ease-of-use. However, its size and weight are not appropriate for longer deployment. Instead of using a passive balancing system for the handheld device or even a separate cooperating robot placed next to the OR table, as both approached would be bulky and space consuming, we decided to develop a new system worn at the surgeon's arm near to his or her centre of gravity to improve ergonomic handling. This is intended to lead to a better acceptance of and control over the system by the surgeon.

In the following sections, we will present and describe the system's concept, basic components, the control strategy (all in Section II), first results (Section III), and a conclusion (Section IV).

## II. SYSTEM DESIGN

In this paper, we provide an overview of the BOrEScOPE system. It comprises an external optical high-speed tracking system for six Degrees Of Freedom (DOF), position and orientation measurement fused with data from an Inertial Measurement Unit (IMU), the robotic system including actuation and sensor systems together with the mechanical part, the control hard- and software, and finally an opto-acoustic display unit for interactive user guidance. In the following sections, we will address these sub-systems and describe the control strategy.

### A. Robotic System

The robotic system of the BOrEScOPE basically consists of an exoskeleton for the (right) arm of the surgeon including shoulder and wrist (Fig. 1). All together, seven active DOF are realized to provide good compliance with the human anatomy and the same dexterity. The range of motion of the shoulder ( $170^\circ$  abd./add.;  $150^\circ$  flex./ex.;  $180^\circ$  inw./outw. rotation), elbow ( $100^\circ$  flex.), and wrist ( $150^\circ$  pron./sup.;  $20^\circ$  ulnar flex./ex.;  $120^\circ$  flex./ex.) joints has been derived experimentally. Shoulder elevation is not considered as the abduction angle is reduced to  $80^\circ$ . The arm is attached to a backpack that is carried by shoulder and hip harness.

To achieve a lightweight mechanism in the final version, the actuators are placed in the backpack and force is transmitted via Bowden cables. The actuators will be based on the twisted string-concept [21], using a bunch of at least two strings that are twisted axially by a DC motor. This causes the string-arrangement to shorten and produces a

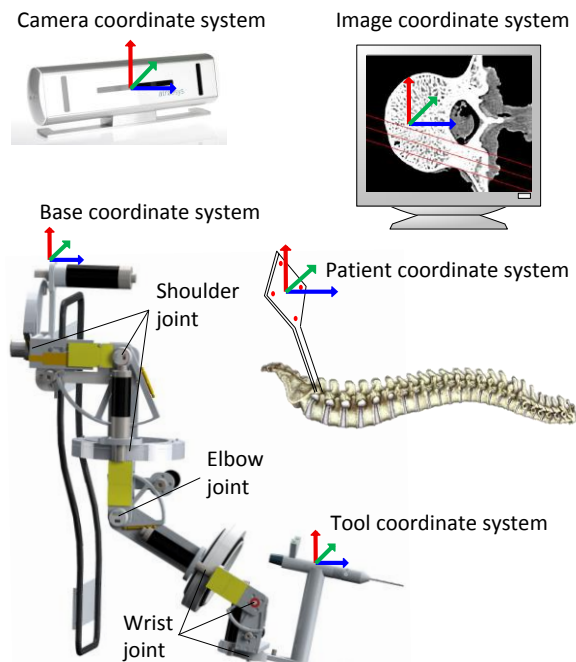


Figure 1. Overview of the robotic sub-system of the BOrEScOPE consisting of the actual exoskeleton, a 3D measurement camera, control computer, and patient (shown as spinal column only).

rather high force. Using a lightweight  $\varnothing 17$  mm DC motor (1741 024 CXR by Faulhaber, Schönaich, Germany) with 8 mNm nominal torque and three strings, a force of 130 N can be produced. Also, no traditional gear reduction is needed leading to very quiet operation.

As only pulling forces can be produced, an antagonistic arrangement is used. Sensors are deployed at the string actuator to measure contraction and at the actuated joint to provide precise angle information. By doing so, the elasticity of the Bowden cable is used to derive a series-elastic actuator (SEA) [22]. Prior work of our group showed good results using SEA in human machine interaction [23]. The inherent compliance allows zero-torque control and robust reaction to dynamic external forces. This reduced stiffness “feels better” than a conventional robotic arm.

The final system will be designed to carry a 2.5 kg payload of a surgical device [24] and compensate the gravity force of the human arm up to a body weight of 80 kg. Shoulder and elbow joints can provide speeds up to 6 rad/s. The static force to guide the user can be up to 10 N at the handle.

### B. Opto-Acoustic Display

One of the challenges in developing a user-friendly Graphical User Interface (GUI) for the Human Machine Interaction (HMI) is to facilitate an intuitive operation and control of the technical system. The basic requirements are to reduce the possible error occurring during user interaction with the machine and to navigate the user. Since the tool position is influenced by the human tremor (frequency range of several Hertz), and since latencies in the feedback-loop must be avoided, a dynamical tool tracking is proposed, consisting of a combination of optical and inertial motion measurements. Based on these data the User Guidance Opto-Acoustic Display (UGOAD) is realized, which navigates the user to the goal pose (position and orientation), displays the processing trajectory, and gives a feedback of pose errors. Display and measurement latency has to be kept low to reduce phase shift in the feedback loop and to provide stable overall system behavior. The goal 6D poses as well as the processing trajectories are provided from planning data, which are defined by the surgeon using 3D patient imaging (CT). According to the requirements, a first UGOAD functional prototype was realized (see Fig. 2).

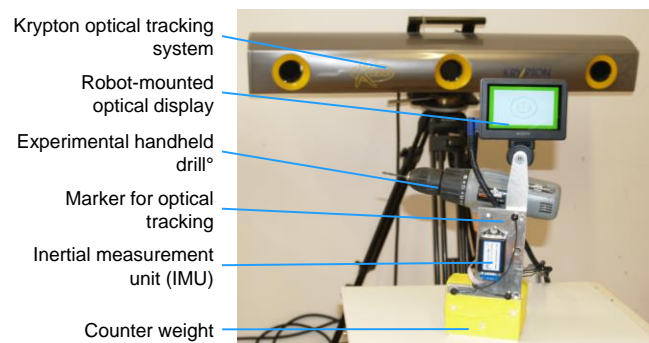


Figure 2. Experimental environment for the first handheld prototype of the opto-acoustic display (UGOAD) deployed in the BOrEScOPE system.

The experimental handheld drilling tool (Fig. 2), on the left) was equipped with three active optical LED markers and an IMU device (Crista IMU, Cloud Cap Technology, Inc.). The miniature monitor (Fig. 2, on the right) mounted at the distal end of the system can provide both optical and acoustic information. In the final implementation, a lightweight miniaturized screen will be attached directly to the tool. The optical tracking system (Krypton K600, Nikon Metrology, Inc.) (Fig. 2, in the background) is used in addition to the Crista IMU to collect the motion data of the handheld device. Data fusion is accomplished using Kalman-filter based methods [25]. The resulting filtered variables for position, orientation, velocities, angular rates, and linear acceleration are utilized for navigation purposes and provided to the lower levels. In later development stages the display can be mounted and aligned to the exoskeleton. The 6 DOF user navigation is realized by 2D representations of the tool pose on the UGOAD which is described below in detail.

### C. Control Structure

The control system is developed according to Nested Recursive Behavior-based Control (RNBC) structure [26]. Accordingly, the hardware is realized as a number of components (Fig. 3) interacting on diverse behavioral levels. In contrast to a one-to-one mapping of the behavior levels, one single behavior level can be distributed on multiple hardware components. Several behavior levels may be aggregated in one single hardware device. In the latter case, behaviors are realized as software processes. For the BOReSCOPE realization, the upper levels, i.e., *mission*, *navigation* and *trajectory control*, are realized as software

processes integrated into a QNX-based (QNX Software Systems Ltd.) real-time PC. The behavior levels for *position control*, *collision avoidance*, *velocity control* and *force control* are realized using an embedded PC based on xPC Target™ (The Mathworks, Inc.). The xPC™ Target PC is interconnected with the QNX PC via a serial link and to the motor controllers (type EL7342 by Beckhoff Automation, Verl, Germany) via EtherCAT. The motor controllers directly control the currents of the actuators. Position constraints for link actuation are calculated using the robot kinematics in order to avoid internal collisions. Additionally, external ultrasonic (US) sensors can help to avoid collisions of the robot with its environment. A milling tool can be aligned with the patient coordinate frame and a target bone can be processed with the preplanned trajectory.

To achieve compliance with the behavior of the operator, three interaction modalities are realized: The opto-acoustic display provides optical (1) and acoustical output (2) while the robot provides haptic feedback (3). The control algorithm's input is a virtual static force field generated around the main axis of the bore and depending on the actual distance, speed and direction of movement of the BOReSCOPE's end effector [27, 28]. When the patient is moving, this force field also moves in space. To achieve smooth and comfortable movement, the real force acting between BOReSCOPE and the wrist are measured. The user tries to minimize the forces following the BOReSCOPE system.

Using this algorithm, the 7 DOF redundant robotic system can be controlled easily and intuitively while maintaining

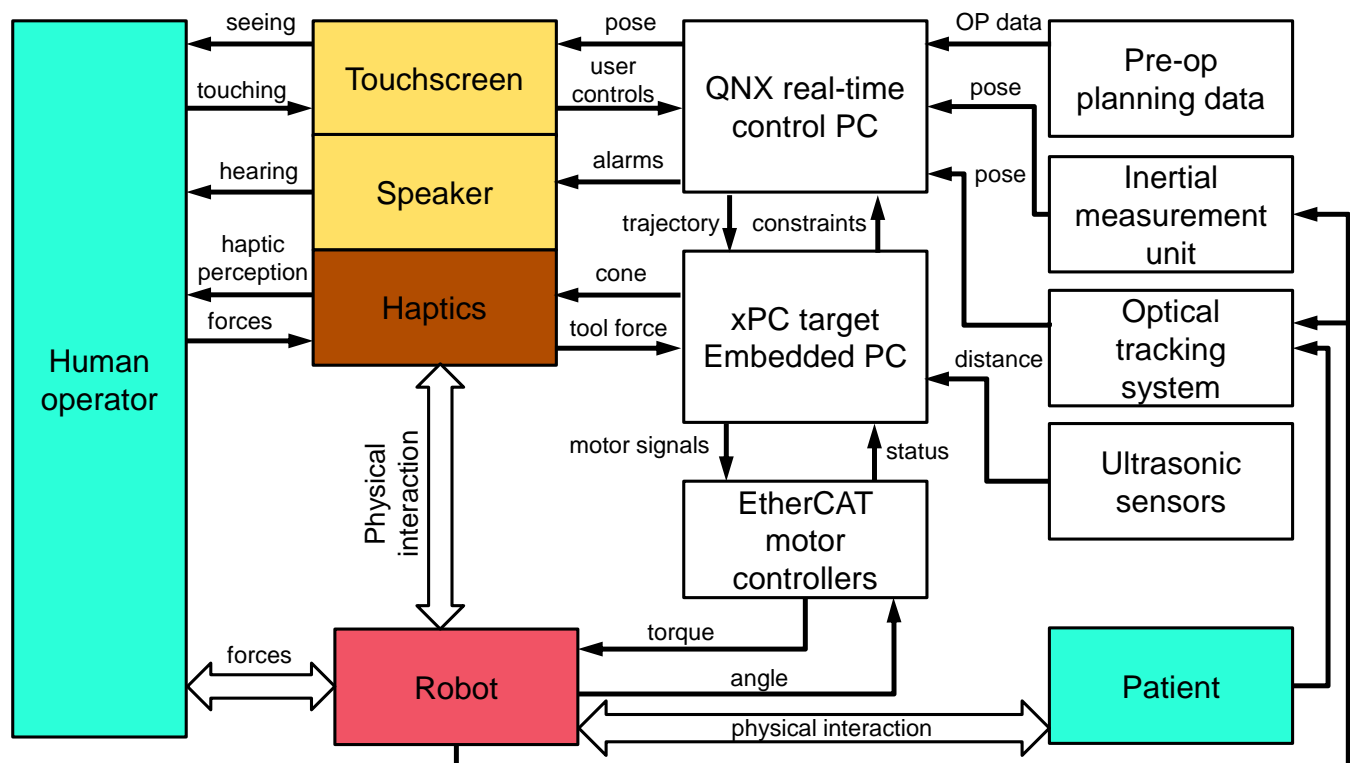


Figure 3. System architecture of the BOReSCOPE system. The human operator interacts with the robotic system, which interacts with the patient. This latter interaction is measured by a number of sensors while the first is based on audio, visual, and haptic effects.



Figure 4. First Prototype of the BOrESCOPE system as a CAD drawing.

the human's dexterity. As both, the linear displacement at the actuators and the angular displacement in the actual joints are measured and controlled, serial-elastic actuation is achieved.

### III. RESULTS

The BOrESCOPE system is still under development. The two main sub-systems *opto-acoustic display* and *robotic system* show first and promising results that are described in the following.

#### A. Robotic System

The mechanical sub-system of the BOrESCOPE is shown in Fig. 4. The device features the same seven axes as a human arm and can be adjusted to persons between roughly 165 and 200 cm body height and a BMI under 30. It is worn around the arm and thus provides congruent axes. To allow this for the axial rotation of upper and lower arm, special wire ball bearings (LEL 1.5/5 by Franke GmbH, Aalen,

Germany) have been chosen for a lightweight, strong, and backlash-free solution for these two DOF. For first experiments, conventional DC gear-motors (shoulder joint: 3890 048 CR+38/2 S, elbow joint: 3272 048 CR+32/3 S, wrist joint: 2657 048 CR+26/1 S) and wire-gearing have been chosen to reduce development effort while still accounting for backlash-free smooth motion with constant friction. The range of motion of the shoulder ( $100^\circ$  abd./add.;  $90^\circ$  flex./ex.;  $180^\circ$  inw./outw. rotation), the elbow ( $105^\circ$  flex.) and wrist ( $150^\circ$  pron./sup.;  $35^\circ$  ulnar flex./ex.;  $90^\circ$  flex./ex.) fits in the requirements of the operational task. Its force is capable to maneuver payload up to 1 kg safely within the complete range of motion. The device can be worn by the surgeon using a backplate and a rucksack-like arrangement of straps and belts.

A first realization of the 3-DOF wrist of the robot is shown in Fig. 5. Here, especially the wire-gearred actuation principle and the structural integration of the torque sensors is visible. The structural integration allows high-stiffness measurement with no additional masses or elasticity. It is achieved by integrating full-bridge strain gauges to the wire-gearing mechanism in a way that the pulling force of the wire is measured.

#### B. Opto-Acoustic Display

The measured peak response time of hand movement as a result of optical stimuli amounts to around 250 ms. The requirement of visually provided information should be adapted on this process time. The reaction time of the UGOAD as well as the robot must be kept within a limit of 10-20 ms (10 to 20-fold faster). Thus, the calculation of graphical contents and of the control algorithm should terminate within this time. Based on this knowledge, the sensor data acquisition, the global-control loop, and UGOAD were implemented as real-time processes in the QNX Neutrino operating system.

The first display prototype was realized by a 2D representation of the 6 DOF pose data. Accordingly, the actual and the reference pose of the tool are shown in the x-y-plane of the display. The z-axis is perpendicular to the display plane. In order to intuitively capture the 6 DOF contents in the 2D image a two body projection metaphor is

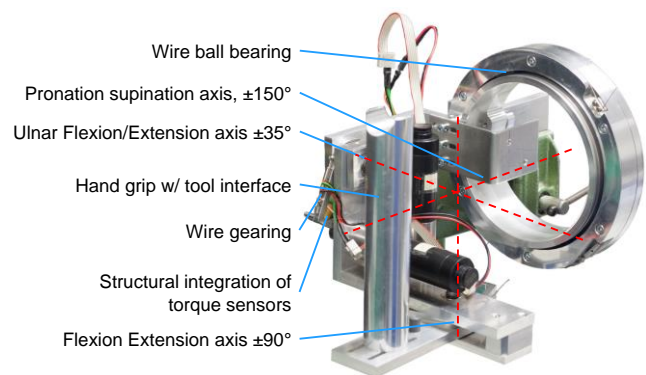


Figure 5. First realisation of the wrist. The three axes intersect in one point in the centre of the human wrist (not shown).

realized. In this imagination one small colored octagon is mounted virtually at the tool tip and one large colored octagon at the rear of the tooling machine. Looking from above in direction of the drilling tool (z-axis) corresponds to looking through the large octagon and through the small octagon on the tool tip, which is in the center of both. The small black octagon with crosshairs and large black octagon are virtually mounted at the target (reference) pose. If the tool is aligned (Fig. 6a), the small octagons are aligned and the large colored octagon has its original size in the central position. If the tool is misaligned in the x-axis (Fig. 6b) the large colored octagon is shifted correspondingly in the x-direction. The same holds for the y-axis. A misalignment in the z-axis is represented by the size of the large colored octagon. A deviation in the positive z-direction means that the tool is too far away from the user, which is shown by the reduced size relatively to the large black octagon. Negative deviation displays an increased size of the octagon to report that the tool is too narrow. A deviation in the orientation is displayed as shift of the small colored octagon. For example, if the tool is turned around the y-axis (Fig. 6), the tool tip is moved in x-direction, displayed as x-axis-shift of the small colored octagon. The corresponding principle holds for the orientation error around the x-axis. Here, a y-shift of the small octagon can be observed. The orientation error around the z-axis is directly displayed as a rotation of the colored octagons around their centers.

As additional element, a rectangular border is shown in green color, which indicates that the pose is in the desired workspace. If the tool approximates the limit positions for at least one axis, the color changes firstly from green to orange, showing that a user intervention is required. In critical vicinity to the constraints the color changes to red (Fig. 6d) asking for urgent motion actions. The color change is supported by changing the waveform of the acoustic channel.

### C. User Experiments

Several experiments with subjects (users) have been performed resulting in a first performance test of the UGOAD. The goal was to keep the handheld drill (Fig. 2) still in position and orientation in six DOF while looking at the UGOAD only and at the tool-tip exclusively in guided (assisted) and unguided (unassisted) case, respectively. The user himself chose the holding comfortable pose. Substantial results of these trials are presented for two users exemplary.

#### User1:

The first human operator (user 1) was requested twice to hold the tool calmly during 60 seconds. Firstly, without UGAOD assistance and secondly after short instruction and training with the UGOAD. The results point out that it was possible to keep the tool in the defined workspace ( $\pm 5$  mm in position-axes and  $\pm 5^\circ$  in orientation-axes) in assisted attempt (blue trajectory, Fig. 7). Unassisted the workspace was left after short time and the trajectory was drifted in all axes (red trajectory, Fig. 7). To evaluate the position errors the histo-

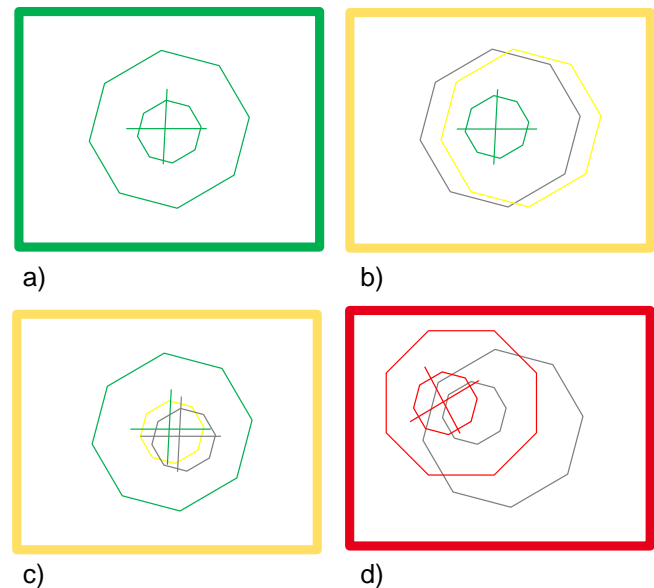


Figure 6. Display content of the UGOAD (refer to Fig. 2): a) Correct position and orientation, b) Translational displacement in x-axis, c) Rotational displacement around x- and y-axis, d) Displacement in all view axes.

grams for both cases with and without UGOAD are represented in one plot (Fig. 8).

Without assistance, the position is distributed over a wide range according to the non-stationary process. With UGOAD feedback the human-in-the-loop position control reaches as stationary condition, while the remaining position error has a distribution with an approximately Gaussian

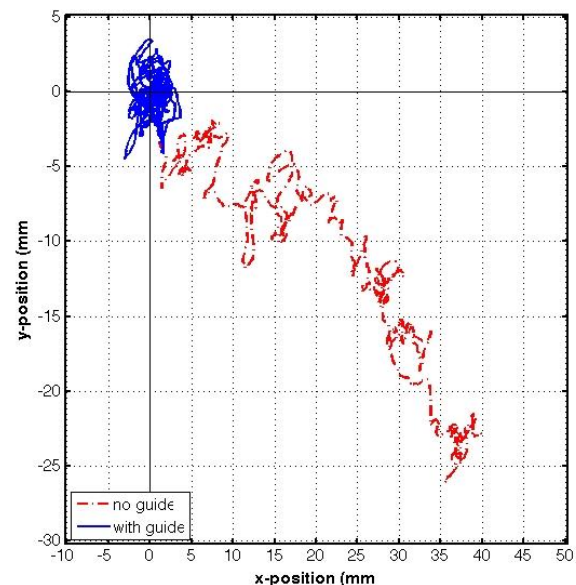


Figure 7. Position deviation in xy-direction with and without guide with the human operator (user1) in the loop (without the robotic sub-system). z-axis deviation is not shown for reasons of brevity.

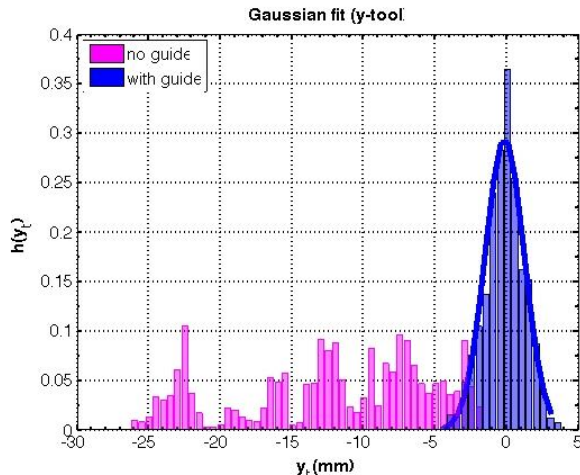


Figure 8. Position y-deviation histogram for guided and unguided trial of user1 (instructed).

shape. The histograms show the posed distribution together with a fit using the normal distribution in one dimension while the standard deviation and the mean of the distribution are  $\sigma = 1.3529$  and  $\mu = -0.2039$  for the case with UGOAD and  $\sigma = 6.606$  and  $\mu = -12.0661$  for the case without UGOAD, respectively.

User2:

Another human operator (user 2) was also requested twice to hold the tool also calmly during 60 seconds. In both cases, the UGOAD was used. In contrast to the former experiment, user2 was not instructed about the operating principle of the UGOAD so that the user had to find it out by himself during trial 1. Nevertheless, it was possible to keep the tool inside the workspace (blue trajectory, Fig. 9). The second trial shows the learning effect in operation (red trajectory, Fig. 9).

The histograms show also Gaussian shapes for both trials with UGOAD while the standard deviation and the mean of the distribution are  $\sigma = 1.8460$  and  $\mu = -3.9976$  for trial 1 and  $\sigma = 0.8879$  and  $\mu = -0.4686$  for trial 2, respectively (Fig. 10).

It is obvious that using the opto-acoustic display a strong improvement of the pose deviation was achieved (here presented for two different axes and operators).

#### IV. DISCUSSION AND CONCLUSION

To set up a robotic system with close human-machine interaction in a medical environment is a delicate task. However, the project is still in progress and work starting from the presented concept to the final realization is still ongoing. We managed to define interfaces between the robotic system and the human operator not only mechanically, but also visually and using the audio channel. Smooth and comfortable working with the system is strongly dependent on low latency, high update rates, and actually predictable behavior. Here, our system will have to deal with some drawbacks as the force field generation is depending on data quality of the optical tracking system which tends to

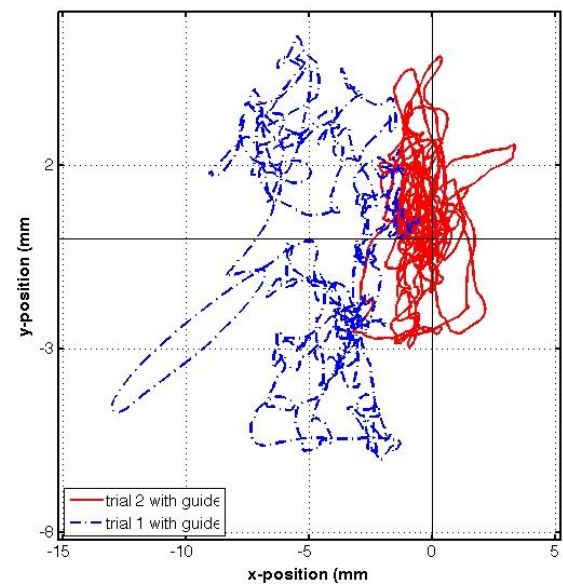


Figure 9. Position deviation in xy-direction for two trials with guide with the human operator (user2) in the loop (without the robotic sub-system).

jitter and noisy signals. This will be addressed in future by using redundant LED markers and by combining data of an inertial tracking system. Furthermore, the quality of real-time data transfer will be improved.

Mechanically, the robot will have to cope with force-depended friction wire gearing and residual backlash in the gearing. This issue will be addressed by a model-based controller with individual parameters for each axis. The first prototype shown in Fig. 4 differs slightly from the initial concept due to time restriction during development. However, the schedule of the first tests of the complete system is set and first promising objectives have been reached.

First experiments with users demonstrate that the 6 DOF-guidance can be captured by the majority of subjects

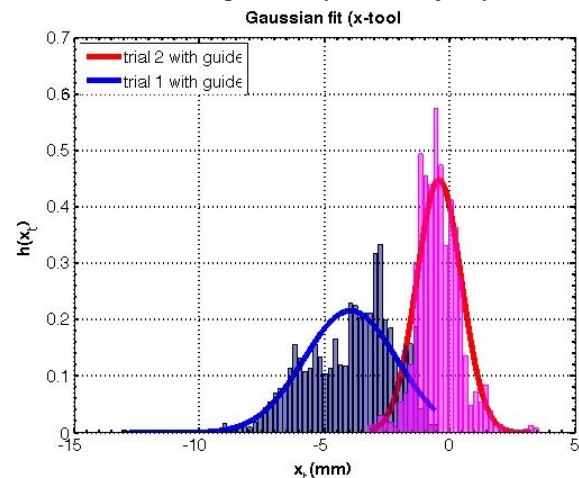


Figure 10. Position x-deviation histogram for guided trials of user2 (uninstructed).

without further explanation (Fig. 6). Thus, the usage of the UGOAD as a feedback in the human interaction with the machine implicates a massive improvement of human performance to achieve the common tasks and there is every indication that the developed UGOAD insure an intuitive operation and an intuitive control.

#### ACKNOWLEDGMENT

The work is funded by the German Federal Ministry of Education and Research under grants 16SV5773 and 16SV5774.

#### REFERENCES

- [1] P. P. Pott, M. Hessinger, R. Werthschützky, H. F. Schlaak, E. Nordheimer, E. Badreddin, and A. Wagner, "BOrESCOPE – Exoskeleton for Active Surgeon Support during Orthopedic Surgery," Proc. 7. International Conference on Advances in Computer-Human Interactions (ACHI 2014), Barcelona, pp. 377-380, 2014.
- [2] P. P. Pott, H.-P. Scharf, and M. L. R. Schwarz, "Today's State of the Art of Surgical Robotics," Journal of Computer Aided Surgery, vol. 10, pp. 101-132, 2005.
- [3] Y. Kwok, I. Reed, J. Chen, H. Shao, T. Truong, and E. Jonckheere, "A new computerized tomography-aided robotic stereotaxis system," Robotics Age, pp. 17-22, 1985.
- [4] J. Doll, W. Schlegel, O. Pastyr, V. Sturm, and W. Maier-Borst, "The use of an industrial robot as a stereotactic guidance system," Proc. International Symposium and Exhibition on Computer Assisted Radiology (CAR 87), Berlin, D, 1987.
- [5] R. H. Taylor, *et al.*, "An Image-Based Robotic System for Hip Replacement Surgery," Journal of the Robotics Society of Japan, pp. 111-116, 1990.
- [6] C. Caetano da Rosa, Operationsroboter in Aktion. Bielefeld, Germany: transcript Verlag, 2013.
- [7] K. Cleary and C. Nguyen, "State of the art in surgical robotics: Clinical Applications and Technology Challenges," Computer aided Surgery, vol. 6, pp. 312-328, 2001.
- [8] R. Taylor and D. Stoianovici, "Medical Robotics in Computer-Integrated Surgery," IEEE Transactions on Robotics and Automation, vol. 19, pp. 765-781, 2003.
- [9] K. Cleary, D. Stoianovici, V. Watson, R. Cody, B. Hum, and D. Lindisch, "Robotics for Percutaneous Spinal Procedures: Initial Report," Proc. Computer Aided Radiology and Surgery, San Francisco, USA, 2002.
- [10] W. Korb, R. Marmulla, J. Raczowsky, J. Mühling, and S. Hassfeld, "Robots in the operating theatre—chances and challenges," Int. J. Oral Maxillofac. Surg., vol. 33, pp. 721-732, 2004.
- [11] F. Cepolina, B. Challacombe, and R. C. Michelini, "Trends in robotic surgery," J Endourol, vol. 19, pp. 940-51, Oct 2005.
- [12] C.-H. Kuo and J. S. Dai, "Robotics for Minimally Invasive Surgery: A Historical Review from the Perspective of Kinematics," in *International Symposium on History of Machines and Mechanisms*, H.-S. Yan and M. Ceccarelli, Eds., ed: Springer Science+Business Media B.V., 2009, pp. 337-354.
- [13] V. Vitiello, S.-L. Lee, T. Cundy, and G.-Z. Yang, "Emerging Robotic Platforms for Minimally Invasive Surgery," IEEE reviews in Biomedical Engineering, vol. 6, pp. 111-126, 2013.
- [14] P. W. Dhumane, M. Diana, J. Leroy, and J. Marescaux, "Minimally invasive single-site surgery for the digestive system: A technological review," J Minim Access Surg, vol. 7, pp. 40-51, 2011.
- [15] M. Jakopec, S. J. Harris, F. R. Baena, P. Gomes, J. Cobb, and B. L. Davies, "The First Clinical Application of a "Hands-on" Robotic Knee Surgery System," Computer Aided Surgery, vol. 6, pp. 329-339, 2001.
- [16] H. Mayer, I. Nagy, A. Knoll, E. U. Schirmbeck, and R. Bauernschmitt, "A robotic system providing force feedback and automation for minimally invasive heart surgery," Proc. 20th International Congress and Exhibition on Computer Assisted Radiology and Surgery CARS 2006, Osaka, Japan, pp. 265-267, 2006.
- [17] M. Shoham, M. Burman, E. Zehavi, and Y. Kunicher, "MARS: miniature bone-mounted robot," Proc. ISRAELAS'2003, Tel Aviv, Israel, 2003.
- [18] P. P. Pott, *et al.*, "ITD - A handheld manipulator for medical applications - Concept and design," Proc. 3rd annual meeting of CAOS, Marbella / Spain, pp. 290-291, 2003.
- [19] P. P. Pott, A. Wagner, E. Badreddin, H.-P. Weiser, and M. L. R. Schwarz, "Inverse Dynamic Model and a Control Application of a Novel 6-DOF Hybrid Kinematics Manipulator," Journal of Intelligent and Robotic Systems, vol. 63, pp. 3-23, 2010.
- [20] A. El-Shenawy, A. Wagner, P. P. Pott, and E. Badreddin, "Disturbance Attenuation of a Handheld Parallel Robot," Proc. IEEE ICRA, Karlsruhe, 2013.
- [21] T. Würtz, C. May, B. Holz, C. Natale, G. Palli, and M. C., "The Twisted String Actuation System: Modeling and Control," Proc. IEEE/ASME International Conference on Advanced Intelligent Mechatronics, Montréal, Canada, pp. 1215-1220, 2010.
- [22] K. Kong, J. Bae, and M. Tomizuka, "Control of Rotary Series Elastic Actuator for Ideal Force-Mode Actuation in Human-Robot Interaction Applications," IEEE/ASME Transactions on Mechatronics, vol. 14, pp. 105-118, 2009.
- [23] M. Grün, R. Müller, and U. Konigorski, "Model Based Control of Series Elastic Actuators," Proc. IEEE Biomedical Robotics and Biomechatronics (BioRob), Rome, Italy, pp. 538-543, 2012.
- [24] M. Hessinger, J. Hielscher, P. P. Pott, and R. Werthschützky, "Handheld surgical drill with integrated thrust force recognition," Proc. E-Health and Bioengineering Conference (EHB), Iasi, RO, 2013.
- [25] N. Sadaghzadeh, L. Zouaghi, A. Wagner, J. Poshtan, and E. Badreddin, "Cascaded Error Estimation and Compensation of an Inertial Measurement Unit using the Fusion of Optical and Inertial Sensors," Proc. COMADEM, Helsinki, 2013.
- [26] E. Badreddin, "Recursive Control Structure for Mobile Robots," Proc. International Conf. on Intelligent Autonomous Systems 2 (IAS.2), Amsterdam, pp. 11-14, 1989.
- [27] A. Wagner, E. Nordheimer, and E. Badreddin, "Hierarchical constraint-based singularity avoidance," Proc. System Theory, Control and Computing (ICSTCC), Sinaia, 2012.
- [28] O. Khatib, "Real-time obstacle avoidance for manipulators and mobile robots," The International Journal of Robotics Research, vol. 5, pp. 90-98, 1986.